European Journal of Taxonomy 997: 28–50
https://doi.org/10.5852/ejt.2025.997.2919
ISSN 2118-9773
www.europeanjournaloftaxonomy.eu
2025 · Chang K. & Shih H.-T.

Research article

urn:lsid:zoobank.org:pub:2C6ACBDC-658A-49AB-A517-3EE02514E944

Description of a new brittle star of the genus *Breviturma* (Ophiuroidea: Ophiocomidae), with a new record from Taiwan

Kai CHANG [1] & Hsi-Te SHIH [2,*]

[1,2] Department of Life Sciences, National Chung Hsing University, Taichung 402, Taiwan.
[2] Global Change Biology Research Center, National Chung Hsing University, Taichung 402, Taiwan.

[*] Corresponding author: htshih@dragon.nchu.edu.tw
[1] Email: kai.chang.kevin@gmail.com

[1] urn:lsid:zoobank.org:author:41CEBA94-0796-4439-97BC-745C5F4673E7
[2] urn:lsid:zoobank.org:author:A5B6B75B-F554-4E89-B473-452F5AD97B67

Abstract. The genus *Breviturma*, a group of brittle stars inhabiting intertidal and shallow subtidal zones, includes eight recognized species distributed mainly across the Indo-West Pacific. This study describes a new species, *Breviturma securis* sp. nov., from Taiwan. The new species is distinguishable from its congeners through both morphological and molecular evidence, including disc granule density, arm spine sequences, and distinctive color patterns on the dorsal disc and dorsal arm plates. Phylogenetic analyses based on 16S rRNA and COI genes support its unique status, revealing interspecific divergence distances of 18.27–26.66% between *B. securis* and other congeners in the Indo-West Pacific. Based on the distribution patterns of its congeners, *B. securis* is expected to be widely distributed in other regions of the Indo-West Pacific. A newly recorded species, *Breviturma krohi* (Stöhr, Boissin & Hoareau, 2013), from Taiwan is also reported.

Keywords. *Breviturma securis* sp. nov., *Breviturma krohi*, East Asia, 16S rDNA, cytochrome c oxidase subunit I (COI).

Chang K. & Shih H.-T. 2025. Description of a new brittle star of the genus *Breviturma* (Ophiuroidea: Ophiocomidae), with a new record from Taiwan. *European Journal of Taxonomy* 997: 28–50.
https://doi.org/10.5852/ejt.2025.997.2919

Introduction

Breviturma was originally established as a subgenus of the genus *Ophiocoma* Agassiz, 1836 by Stöhr *et al.* (2013) to include species formerly belonging to the "*brevipes* group" (i.e., *Ophiocoma brevipes* Peters, 1851, *O. dentata* Müller & Troschel, 1842, and *O. doederleini* De Loriol, 1899) as defined by Devaney (1970). Stöhr *et al.* (2013) reviewed the *brevipes* group and described a new species, *O.* (*B.*) *krohi* Stöhr, Boissin & Hoareau, 2013. In O'Hara *et al.* (2018), this subgenus was elevated to generic level. Furthermore, species in the "*pica* group" (i.e., *O. longispina* H.L. Clark, 1917, *O. pica* Müller & Troschel, 1842, and *O. pusilla* (Brock, 1888)) as defined by Devaney (1970) as well as

O. paucigranulata Devaney, 1974 were reclassified from *Ophiocoma* to *Breviturma* based on molecular evidence (O'Hara *et al.* 2019). Hence, this genus currently contains eight valid species.

Most species of *Breviturma* are widely distributed in the tropical and subtropical regions of the Indo-West Pacific, with only *B. paucigranulata* found in the Caribbean Sea (Devaney 1970, 1974; Clark & Rowe 1971; Stöhr *et al.* 2013). Three species of *Breviturma*, *B. brevipes*, *B. dentata*, and *B. pica*, have been recorded in Taiwan, including the Penghu Archipelago, Siaoliouciou, and Lanyu (Orchid Island). All were found in intertidal and shallow subtidal zones of rocky shores or coral reefs (Applegate 1984; Chao *et al.* 1991; Hung 2000; Chao 2002; Huang & Lee 2021; Shih *et al.* 2023).

Research on ophiuroids in Taiwan has been limited, particularly since the study by Chao (2002). Although some recent studies have been published (e.g., Huang & Lee 2021; Shih *et al.* 2023), over two decades have passed without comprehensive taxonomic assessments concerning Taiwanese ophiuroids. This study contributes to knowledge of ophiuroid diversity by describing a new species and reporting a new record of *Breviturma*, utilizing both morphological and molecular evidence.

Material and methods

Institutions acronyms

NCHUZOOL = Zoological Collections of the Department of Life Sciences, National Chung Hsing University, Taichung, Taiwan
NMNS = National Museum of Natural Science, Taichung, Taiwan

General abbreviations

ASp = arm spine
DAP = dorsal arm plate
DD = disc diameter
L = length
OS = oral shield
W = width

Sample collection and preservation

Specimens of *Breviturma* spp. were collected from several localities from Taiwan (Table 1; Fig. 1) and preserved in 95% ethanol after being anesthetized with a $MgCl_2$ seawater solution. All specimens were deposited in NCHUZOOL. In addition, specimens from NMNS were also examined.

Morphological data

The disc granules, oral shields, dorsal arm plates, and arm spines were examined and measured using a stereo microscope (Stemi SV 6, ZEISS) equipped with an HDMI camera (XCAM4K, ToupTek). Detailed morphological traits were assessed as follows: the density of granules on the dorsal central disc was counted within an area of 1 mm²; the length-to-width ratio of the oral shied was measured; the 15th arm segment was selected to determine the width-to-length ratio of the dorsal arm plate, and the proportion of the length of the second dorsalmostarm spine to that of the first dorsalmost arm spine was also calculated. The measured values mentioned above were analyzed for correlation with DD using Pearson's correlation coefficient (r) and Linear Regression Model. All statistical analyses were performed using SAS ver. 9.4 (SAS Institute Incorporation 2013).

One of the paratypes was selected to obtain the ossicles. The specimen was immersed in a 12% NaOCl solution to dissolve the skin and muscle tissue. Afterward, the ossicles were collected, washed with distilled water, and dried in an oven at 40°C. The dried ossicles were mounted on aluminum stubs with

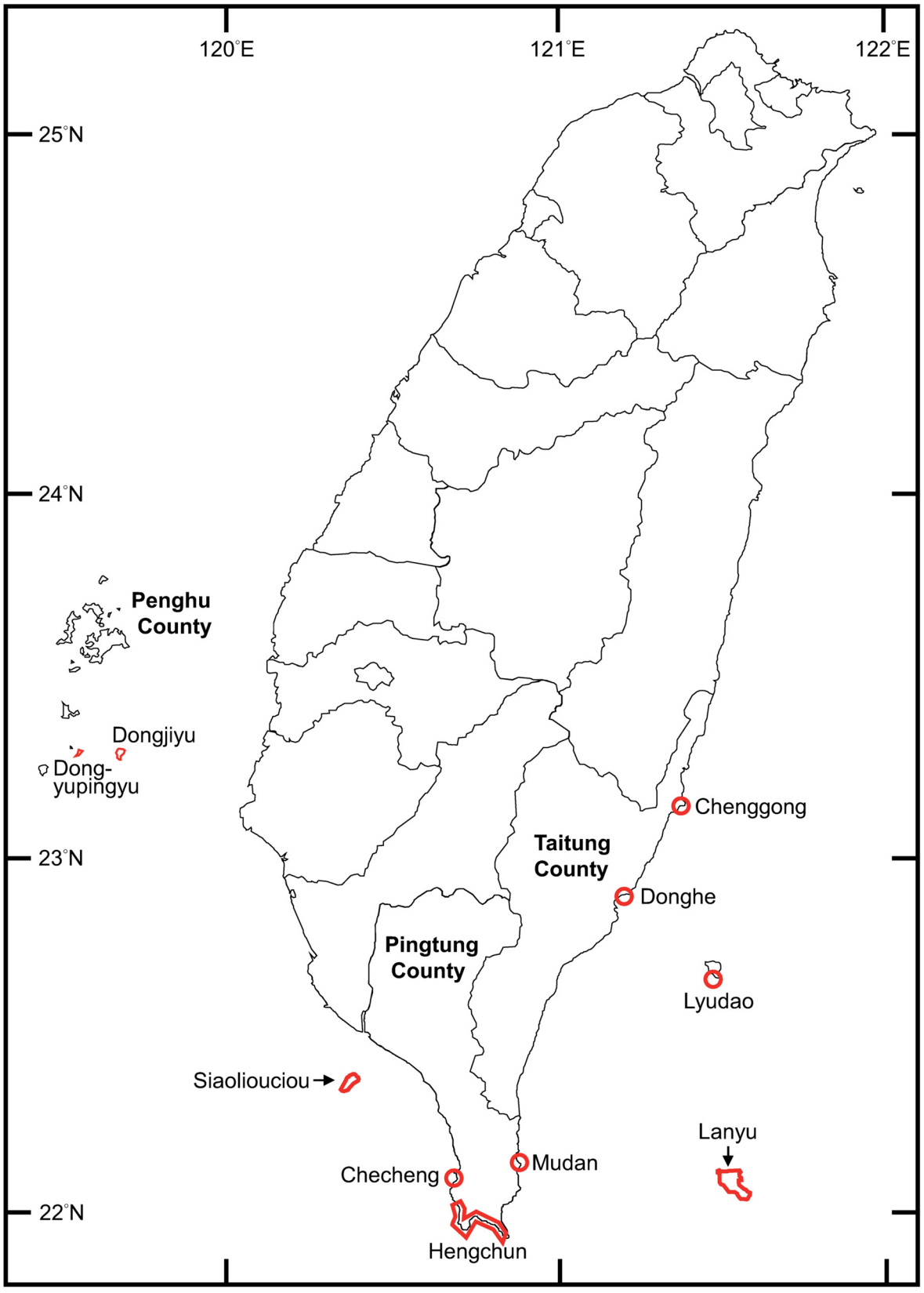

Fig. 1. Collection sites of species of *Breviturma* Stöhr, Boissin & Hoareau, 2013, shown as red empty circles and red outlines, on Taiwan's main island and its offshore islets.

Table 1 (continued on next page). Specimens and 16S, COI haplotypes of species of *Breviturma* Stöhr, Boissin & Hoareau, 2013 used in this study. Sequences available from GenBank were marked with *.

Species	Locality	Catalog no. NCHUZOOL (unless indicated)	16S Haplotype	16S Access. no.	COI Haplotype	COI Access. no.
B. brevipes	Taiwan, Penghu, Dongyupingyu	17279	Bb1	PV166621	BbC1	PV165750
	Taiwan, Taitung, Lanyu	17278	Bb2	PV166620	BbC2	PV165749
B. dentata	Taiwan, Penghu, Dongyupingyu	17283	Bde1	PV166626	BdeC1	PV165755
	Taiwan, Pingtung, Siaoliouciou	17281	Bde2	PV166623	BdeC2	PV165752
	Taiwan, Pingtung, Hengchun	17282	Bde3	PV166625	BdeC3	PV165754
	Taiwan, Pingtung, Hengchun	17282	Bde4	PV166628	BdeC4	PV165757
	Taiwan, Taitung, Lyudao	NMNS 005750-00014	Bde5	PV166627	BdeC6	PV165756
	Taiwan Taitung, Lanyu,	17280	Bde6	PV166622	BdeC5	PV165751
	Taiwan, Taitung, Lanyu	17344	Bde7	PV166624	BdeC7	PV165753
B. doederleini	France, Reunion Island	–	Bdo	KF662939*	BdoC	KF662924*
B. krohi	Taiwan, Penghu, Dongjiyu	17274	Bk1	PV166636	BkC1	PV165765
	Taiwan, Penghu, Dongjiyu	17275	Bk2	PV166638	BkC2	PV165767
	Taiwan, Pingtung, Siaoliouciou	17258	Bk3	PV166631	BkC3	PV165760
	Taiwan, Pingtung, Hengchun	17273	Bk4	PV166641	BkC4	PV165770
	Taiwan, Pingtung, Mudan	17272	Bk5	PV166640	BkC5	PV165769
	Taiwan, Taitung, Chenggong	17260	Bk6	PV166634	BkC6	PV165763
	Taiwan, Taitung, Chenggong	17260	Bk7	PV166630	BkC7	PV165759
	Taiwan, Taitung, Lanyu	17266	Bk8	PV166635	BkC8	PV165764
	Taiwan, Taitung, Lanyu	17261	Bk9	PV166633	BkC9	PV165762
	Taiwan, Taitung, Lanyu	17263	Bk10	PV166632	BkC10	PV165761
	Taiwan, Taitung, Lanyu	17259	Bk11	PV166629	BkC11	PV165758
	Taiwan, Taitung, Lanyu	17266	Bk12	PV166639	BkC12	PV165768
	Taiwan, Taitung, Lanyu	17265	Bk13	PV166637	BkC13	PV165766
	France, Reunion Island	[holotype]	Bk14	KF662935*	BkC14	KC759787*
B. pica	Taiwan, Taitung, Lanyu	17274	Bpi	PV166653	BpiC	PV165782
B. pusilla	Australia	–	–	–	BpuC	KU895185*
B. securis sp. nov.	Taiwan, Penghu, Dongyupingyu	17256	Bs1	PV166652	BsC1	PV165781
	Taiwan, Penghu, Dongyupingyu	17255	Bs2	PV166647	BsC2	PV165776
	Taiwan, Penghu, Dongyupingyu	17256	Bs3	PV166651	BsC3	PV165780
	Taiwan, Penghu, Dongjiyu	17250	Bs4	PV166650	BsC4	PV165779
	Taiwan, Pingtung, Siaoliouciou	17239	Bs5	PV166643	BsC5	PV165772
	Taiwan, Pingtung, Siaoliouciou	NMNS 005621-00012	Bs6	PV166648	BsC6	PV165777

Table 1 (continued). Specimens and 16S, COI haplotypes of species of *Breviturma* Stöhr, Boissin & Hoareau, 2013 used in this study. Sequences available from GenBank were marked with *.

Species	Locality	Catalog no. NCHUZOOL (unless indicated)	16S Haplotype	16S Access. no.	COI Haplotype	COI Access. no.
B. securis sp. nov.	Taiwan, Pingtung, Hengchun	17240	Bs7	PV166645	BsC7	PV165774
	Taiwan, Pingtung, Hengchun	17247	Bs8	PV166646	BsC8	PV165775
	Taiwan, Taitung, Lanyu	17232 [holotype]	Bs9	PV166642	BsC9	PV165771
	Taiwan, Taitung, Lanyu	17234 [paratype]	Bs10	PV166644	BsC10	PV165773
	Taiwan, Taitung, Lanyu	17237 [paratype]	Bs11	PV166649	BsC11	PV165778
outgroups						
O. mixta	South Korea, Jeju Island	–	Om	NC_045937*	OmC	NC_045937*
O. scolopendrina	Taiwan, Penghu, Dongjiyu	17303	Os	PV166654	OsC	PV165783

double-sided adhesive tape and photographed using a scanning electron microscope (SEM, TM 3000 Tabletop Microscope, HITACHI).

Molecular analyses

Genomic DNA was extracted from the tube feet, arm muscle and gonad using the BioKit Tissue & Cell Genomic DNA Purification Kit (Bio-GT150). A portion of the 16S rRNA gene, approximately 490 basepair (bp) in length, was amplified via polymerase chain reaction (PCR) using the universal primers 16Sar and 16Sbr (Palumbi 1991). The cytochrome c oxidase subunit I (COI) gene (655 bp) was amplified using the echinoderm-specific hybrid primers COIceF and COIceR (Hoareau & Boissin 2010). PCR conditions for the primers included 40 cycles of denaturation at 94°C for 50 s, annealing at 46°C for 70 s, and extension at 72°C for 60 s, followed by a final extension at 72°C for 10 min. Sequences were obtained using automated Sanger sequencing (Applied Biosystems 3730xl DNA Analyzer, USA).

Sequences of the different haplotypes were deposited in GenBank (accession numbers are provided in Table 1). Additional sequences of congeners available in GenBank were also included in our analyses. Species of other genera within the same family, including *Ophiomastix mixta* Lütken, 1869 and *Ophiocoma scolopendrina* (Lamarck, 1816), were selected as outgroups, with the former's sequences obtained from GenBank and the latter's from our collection (Table 1). For the GenBank sequences that were shorter than ours or lacked the 16S gene, missing data were designated with '?'. The best-fitting models for sequence evolution of individual datasets in the combined 16S + COI sequences were determined using the Bayesian information criterion (BIC) in PartitionFinder ver. 2.1.1 (Lanfear *et al.* 2017). The selected models, both GTR+G+I, were applied to Bayesian inference (BI) and maximum likelihood (ML) analyses. BI analysis was conducted in MrBayes ver. 3.2.7 (Ronquist *et al.* 2012) with an MCMC run using 4 chains for 10 million generations, sampling every 1000 generations. Convergence of the chains was assessed by achieving an average standard deviation below 0.01, with the first 1400 trees discarded as burn-in. ML analysis was performed in the IQ-TREE ver. 2.3.6 (Minh *et al.* 2020) with 30 000 ultrafast bootstrap replicates. Genetic distances of COI between species, based on Kimura (1980) 2-parameter (K2P) model, were calculated in MEGA ver. 12 (Kumar *et al.* 2024) using the pairwise deletion option.

Results

Systematic account

Class Ophiuroidea Gray, 1840
Order Ophiacanthida O'Hara, Hugall, Thuy, Stöhr & Martynov, 2017

Family **Ophiocomidae** Ljungman, 1867

Diagnosis

The disc ornaments vary among genera: spherical granules in *Ophiocoma* and *Breviturma*, conical granules in *Ophiocomella* A.H. Clark, 1939 and *Ophiomastix* Müller & Troschel, 1842, and slender spines in *Ophiomastix*. Both oral papillae and tooth papillae are present. The dental plate is entire. One or two tentacle scales are present.

Genus ***Breviturma*** Stöhr, Boissin & Hoareau, 2013

Diagnosis

The disc is more or less densely covered with fine, rounded granules, which extend ventrally into the interradial area. Dorsal arm plates are oval or elliptical. The number of arm spines is identical on both sides of the arm. The shape of the arm spines varies among species: slender and elongated in *Breviturma longispina*, *B. paucigranulata*, and *B. pica*; hollow and fragile in *B. pusilla*; short and thick in *B. brevipes*, *B. dentata*, *B. doederleini*, and *B. krohi*. Two tentacle scales are present.

Breviturma securis sp. nov.
urn:lsid:zoobank.org:act:C8B521E9-09DA-4D3B-98C6-8AB7C388E0FD
Figs 2–4

Ophiocoma brevipes – Chao *et al.* 1991: 118–119 (in part), fig. 1c–d. — Hung 2000: 167 (in part), fig. 522. [non *O. brevipes* Peters, 1851].
Breviturma sp. – Ryanskiy 2020: 33, unnumbered fig.
Ophionereis sp. – Ryanskiy 2020: 36, unnumbered fig.
Ophiodermatidae sp. – Ryanskiy 2020: 48, unnumbered fig.
Breviturma aff. *dentata* – Shih *et al.* 2023: 125 (in list).

Diagnosis

The dorsal disc is densely covered with fine granules (Fig. 2C) that extend seamlessly to the ventral side. The oral shields are subequal in length and width (Figs 2D, 3C), while the adoral shields are spear-shaped (Figs 2D, 3D). There are four oral papillae and 10–12 tooth papillae (Fig. 2D). The dorsal arm plates are transversely elliptical (Figs 2E, 3G). The number of arm spines ranges from three to four, with the second dorsalmost arm spines on the 15th–18th arm segments being the longest and exhibiting slightly swollen tips (Fig. 2E–F). The ventral arm plates are pentagonal (Figs 2F, 3H), each bearing two oval tentacle scales on its lateral sides (Fig. 2D, F). The coloration of the dorsal disc is variegated, ranging from yellowish-gray to greenish-gray (Figs 2A, 4), with a dark, axe-shaped central pattern on the dorsal arm plates (Figs 2E, 4). The arms are transversely banded (Figs 2A, 4), with the arm spines showing a light gray base color and irregular, darker annulation (Fig. 2E–F). The ventral side is uniformly light in color (Fig. 2B).

Etymology

The species name *securis* is derived from the Latin word meaning 'axe', referencing the axe-shaped dark patterns on the dorsal arm plates. The name is used as a noun in apposition.

Type material

Holotype

TAIWAN – **Taitung County** • (DD = 14.99 mm); Lanyu, Hongtou; 22°01′19.4″ N, 121°33′29.7″ E; depth < 1 m; 28 Sep. 2022; K. Chang and Y.-C. Hsu leg.; NCHUZOOL 17232.

Paratypes

TAIWAN – **Taitung County** • 1 spec. (DD = 12.00 mm); same data as for holotype; NCHUZOOL 17233 • 3 specs (DD = 8.72–15.74 mm); Lanyu, Hongtou; 22°01′19.4″ N, 121°33′29.7″ E; depth < 1 m; 11 Mar. 2023; K. Chang *et al.* leg.; NCHUZOOL 17234 • 1 spec. (DD = 9.40 mm); Lanyu, Hongtou; 22°01′19.4″ N, 121°33′29.7″ E; depth < 1 m; 22 May 2023; K. Chang *et al.* leg.; NCHUZOOL 17235 • 1 spec. (DD = 4.43 mm); Lanyu, Langdao; 22°04′52.9″ N, 121°32′07.9″ E; depth 7 m; 4 Jul. 2023; K. Chang *et al.* leg.; NCHUZOOL 17236 • 4 specs (1 spec. disc and 1 arm dissected, 4 arms in ethanol) (DD = 10.24–14.70 mm); Lanyu, Dongcing; 22°03′23.1″ N, 121°33′56.8″ E; depth < 1 m; 13 Sep. 2023; K. Chang *et al.* leg.; NCHUZOOL 17237 • 1 spec. (disc broken); Lanyu, Langdao; 22°04′45.3″ N, 121°31′47.9″ E; depth < 1 m; 15 Sep. 2023; K. Chang *et al.* leg.; NCHUZOOL 17238.

Other material examined

TAIWAN – **Penghu County** • 2 specs (DD = 11.77–12.31 mm); Wang'an, Dongjiyu; 23°15′24.9″ N, 119°39′59.4″ E; depth < 1 m; 22 Apr. 2024; K. Chang and Y.-C. Hsu leg.; NCHUZOOL 17248 • 2 specs (DD = 12.85–13.91 mm); Wang'an, Dongjiyu; 23°15′20.5″ N, 119°40′03.1″ E; depth < 1 m; 22 Apr. 2024; K. Chang and Y.-C. Hsu leg.; NCHUZOOL 17249 • 2 specs (DD = 7.67–16.00 mm); Wang'an, Dongjiyu; 23°15′12.0″ N, 119°40′02.9″ E; depth < 1 m; 23 Apr. 2024; K. Chang and Y.-C. Hsu leg.; NCHUZOOL 17250 • 1 spec. (DD = 7.69 mm); Wang'an, Dongjiyu; 23°15′02.9″ N, 119°39′54.0″ E; depth < 1 m; 23 Apr. 2024; K. Chang and Y.-C. Hsu leg.; NCHUZOOL 17251 • 8 specs (DD = 8.07–11.39 mm); Wang'an, Dongjiyu; 23°15′24.9″ N, 119°39′59.4″ E; depth < 1 m; 24 Apr. 2024; K. Chang and Y.-C. Hsu leg.; NCHUZOOL 17252 • 1 spec. (DD = 9.56 mm); Wang'an, Dongjiyu; 23°15′20.5″ N, 119°40′03.1″ E; depth < 1 m; 25 Apr. 2024; K. Chang and Y.-C. Hsu leg.; NCHUZOOL 17253 • 1 spec. (DD = 14.47 mm); Wang'an, Dongyupingyu; 23°15′19.1″ N, 119°30′40.0″ E; depth < 1 m; 26 Apr. 2024; K. Chang and Y.-C. Hsu leg.; NCHUZOOL 17254 • 3 specs (DD = 9.92–13.75 mm); Wang'an, Dongyupingyu; 23°15′21.0″ N, 119°30′45.9″ E; depth < 1 m; 26 Apr. 2024; K. Chang and Y.-C. Hsu leg.; NCHUZOOL 17255 • 5 specs (DD = 12.38–17.65 mm); Wang'an, Dongyupingyu; 23°15′19.1″ N, 119°30′40.0″ E; depth < 1 m; 27 Apr. 2024; K. Chang and Y.-C. Hsu leg.; NCHUZOOL 17256 • 4 specs (DD = 8.58–12.23 mm); Wang'an, Dongyupingyu; 23°15′29.1″ N, 119°30′46.5″ E; depth 1 m; 28 Apr. 2024; K. Chang and Y.-C. Hsu leg.; NCHUZOOL 17257. – **Pingtung County** • 1 spec. (DD = 10.87 mm); Siaoliouciou, Duzaiping; depth < 1 m; 5 Sep. 2007; K.-S. Lee leg.; NMNS 005621-00012 • 2 specs (DD = 9.39–14.15 mm); Siaoliouciou, Shanfu Fishery Harbor; 22°20′24.4″ N, 120°21′46.2″ E; depth < 1 m; 12 Feb. 2023; K. Chang and Y.-C. Hsu leg.; NCHUZOOL 17239 • 6 specs (DD = 8.64–14.61 mm); Checheng, Huangjin Beach; 22°04′52.6″ N, 120°42′06.2″ E; depth < 1 m; 25 Feb. 2024; K. Chang *et al.* leg.; NCHUZOOL 17242 • 2 specs (DD = 13.53–15.23 mm); Hengchun, Nanwan; depth 1 m; 10 Jan. 1991; S.-M. Chao leg.; NMNS 002270-00012 • 1 spec. (DD = 13.38 mm); Hengchun, Tiaoshih, Kenting Great Tide Pool; 26 Jul. 2005; S.-M. Chao and S.-T. Huang leg.; NMNS 004875-00025 • 15 specs (DD = 4.75–15.50 mm); Hengchun, Houbihu; 21°56′18.9″ N, 120°44′43.6″ E; depth < 1 m; 25 Dec. 2023; K. Chang *et al.* leg.; NCHUZOOL 17240 • 7 specs (DD = 3.61–10.98 mm); Hengchun, Wanlitong; 21°59′45.6″ N, 120°42′16.5″ E; depth < 1 m; 26 Dec. 2023; K. Chang *et al.* leg.; NCHUZOOL 17241 • 1 spec. (DD = 9.60 mm); Hengchun, Dingtanzih; 21°55′56.8″ N, 120°44′42.2″ E; depth < 1 m; 26 Feb.

2024; K. Chang *et al.* leg.; NCHUZOOL 17243 • 1 spec. (DD = 8.76 mm); Hengchun, Dingtanzih; 21°55′54.2″ N, 120°44′42.9″ E; depth 8 m; 26 Feb. 2024; K. Chang *et al.* leg.; NCHUZOOL 17244 • 1 spec. (DD = 6.58 mm); Hengchun, Wanlitong; 21°59′44.4″ N, 120°42′22.2″ E; depth < 1 m; 26 Feb. 2024; K. Chang *et al.* leg.; NCHUZOOL 17245 • 5 specs (DD = 3.96–13.93 mm); Hengchun, Wanlitong; 21°59′42.4″ N, 120°42′22.3″ E; depth 5 m; 28 Feb. 2024; K. Chang *et al.* leg.; NCHUZOOL 17247 • 1 spec. (DD = 13.75 mm); Mudan, Gangzaibi; 22°08′49.8″ N, 120°53′32.4″ E; depth < 1 m; 27 Feb. 2024; K. Chang *et al.* leg.; NCHUZOOL 17246. – **Taitung County** • 1 spec. (DD = 11.37 mm); Chenggong, Duli; 23°01′14.7″ N, 121°20′08.0″ E; depth < 1 m; 15 Oct. 2024; K. Chang *et al.* leg.; NCHUZOOL 17338 • 5 specs (DD = 6.42–10.79 mm); Donghe, Dulan; 22°51′51.7″ N, 121°12′34.9″ E; depth < 1 m; 16 Oct. 2024; K. Chang *et al.* leg.; NCHUZOOL 17339.

Comparative material examined

Breviturma brevipes (Peters, 1851)

TAIWAN – **Penghu County** • 1 spec.; Wang'an, Dongjiyu; 23°15′24.9″ N, 119°39′59.4″ E; depth < 1 m; 22 Apr. 2024; K. Chang and Y.-C. Hsu leg.; NCHUZOOL 17289 • 3 specs; Wang'an, Dongyupingyu; 23°15′29.1″ N, 119°30′46.5″ E; depth 1 m; 28 Apr. 2024; K. Chang and Y.-C. Hsu leg.; NCHUZOOL 17279. – **Pingtung County** • 2 specs; Hengchun, Wanlitong; 21°59′42.4″ N, 120°42′22.3″ E; depth 5 m; 28 Feb. 2024; K. Chang *et al.* leg.; NCHUZOOL 17288. – **Taitung County** • 1 spec.; Lanyu, Langdao; 22°04′45.3″ N, 121°31′47.9″ E; depth < 1 m; 25 May 2023; K. Chang and Y.-C. Hsu leg.; NCHUZOOL 17285 • 2 specs.; Lanyu, Longmen Harbor; 22°00′16.5″ N, 121°34′52.7″ E; depth 7 m; 24 May 2023; K. Chang and Y.-C. Hsu leg.; NCHUZOOL 17278 • 1 spec.; Lanyu, Langdao; 22°04′52.9″ N, 121°32′07.9″ E; depth 7 m; 4 Jul. 2023; K. Chang *et al.* leg.; NCHUZOOL 17286 • 1 spec.; Lanyu, Langdao; 22°04′45.3″ N, 121°31′47.9″ E; depth < 1 m; 6 Jul. 2023; K. Chang and Y.-C. Hsu leg.; NCHUZOOL 17287.

Description

Holotype

DD 14.99 mm (Fig. 2A–B). Dorsal disc and radial shields densely covered with spherical granules (279 per mm², Figs 2A, C, 5A), extending ventrally to distal end of oral shields (Fig. 2D). Oral shields subequal in length and width, L/W ca 1.1 (Figs 2D, 5B), broadest mid-part, lateral edges slightly convex, converging distally. Madreporite enlarged, rounded. Adoral shields spear-shaped; adradial edge covered by oral shield, proximal abradial edge slightly concave (Fig. 2D). Four rectangular oral papillae per jaw half, distal-most widest. Lyman's ossicles slender, posterior to distal-most oral papillae. 10–12 rounded tooth papillae on jaw tip (Fig. 2D). Genital slits extend from oral shields to disc margin. Five arms. Dorsal arm plates transversely elliptical, W/L ca 2.2 (Figs 2E, 5C), slightly convergent proximally, straight distally, rounded laterally. Arm spines freestanding, cylindrical, tapering terminally (Fig. 2E–F). Second dorsalmost arm spines on 15th–18th arm segments longest, slightly swollen at tip. Arm spines sequence of proximal 20 segments: 3, 3, 3, 3, 4, 4, 4, 4, 4, 4, 4, 4, 4, 4, 4(3), 4(3), 3, 3, 3, 3. First ventral arm plates rounded-triangular, W > L (Fig. 2D); following plates pentagonal, subequal in width, length, convex distally, proximally lateral edges concave for tentacle scales (Fig. 2F). Two equal oval tentacle scales, slightly longer than wide, arranged in a narrow angle (Fig. 2F).

Ossicles

One paratype, NCHUZOOL 17237. DD = 14.70 mm. Radial shields triangular, with all tips rounded (Fig. 3A). Adradial genital plate bar-like, slightly longer than abradial genital plate, proximal three quarters flattened, thin, distal end thicker, with an articulation for abradial genital plate (Fig. 3B1). Abradial genital plate slightly bended, flattened thoroughly except for distal end (Fig. 3B2). Oral genital plate thin, C-shaped (Fig. 3B3). Oral shields pear-shaped, L/W = 1.4, widest near middle part (Fig. 3C1). Madreporite enlarged, round, distal hole large, one oval hydropore at distal lateral edge (Fig. 3C2). Adoral shields spear-shaped, sharp at distal end, adradial and abradial sides slightly concave (Fig. 3D).

Dental plate outer part with five tooth sockets, dorsalmost two penetrated (Fig. 3E1), outer ventral part with nine small tooth papillae sockets, inner ventral half with five horizontal ridges (Fig. 3E2). Oral plates abradial side with well-defined horizontal muscle flanges (Fig. 3F1), adradial side with strong folds (Fig. 3F2). Dorsal arm plates transversely elliptical, W / L = 1.67, slightly convex distally, proximal lateral edges convergent (Fig. 3G). Ventral arm plates pentagonal, subequal in length and width, distal edge strongly convex, proximal edge with an angle of about 90°, lateral edges with notches on each side for tentacles and tentacle scales (Fig. 3H). Lateral arm plates strongly arched, outer side with four arm spine articulations (Fig. 3I1), inner ventral part with a perforation (Fig. 3I2). Vertebrae subequal in height and width, articulation zygospondylous, dorsal and ventral grooves present, dorsal lateral edge smooth and rounded, ventral lateral edge convergent (Fig. 3J).

Paratypes and non-type variations

Paratypes DD 4.43–15.74 mm, non-types DD 3.61–17.65 mm. Disc granules denser in smaller individuals, reaching 408 / mm² (Fig. 5A). Oral shields ratios stable across all sizes (Fig. 5B). W / L ratios

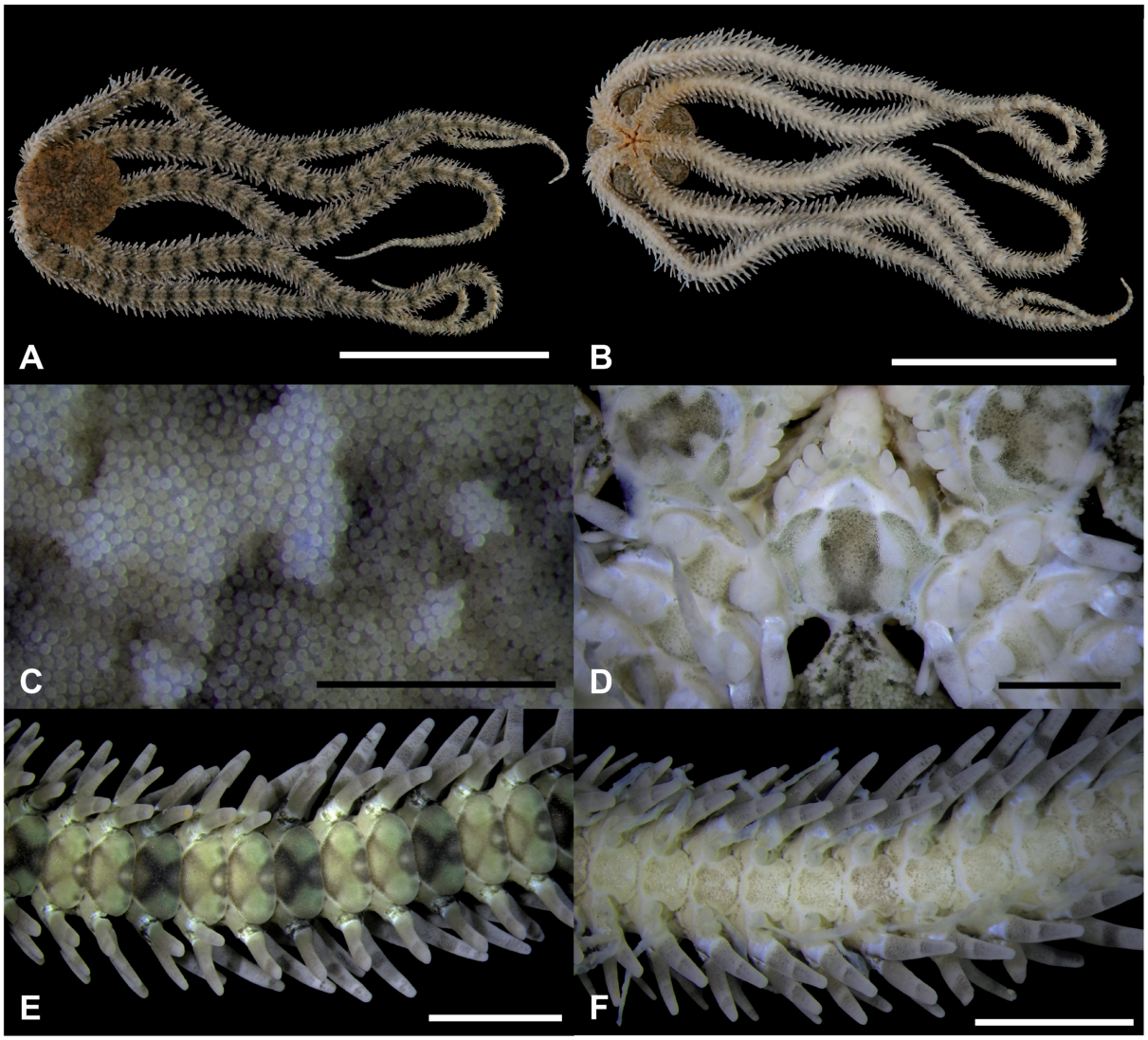

Fig. 2. *Breviturma securis* sp. nov., holotype (NCHUZOOL 17232). **A–B**. Fresh color. **A**. Dorsal. **B**. Ventral. **C–F**. Ethanol preserved color. **C**. Granules on central dorsal disc. **D**. Oral section. **E**. Proximal dorsal arm. **F**. Proximal ventral arm. Scale bars: A–B = 30 mm; C–D = 1 mm; E–F = 3 mm.

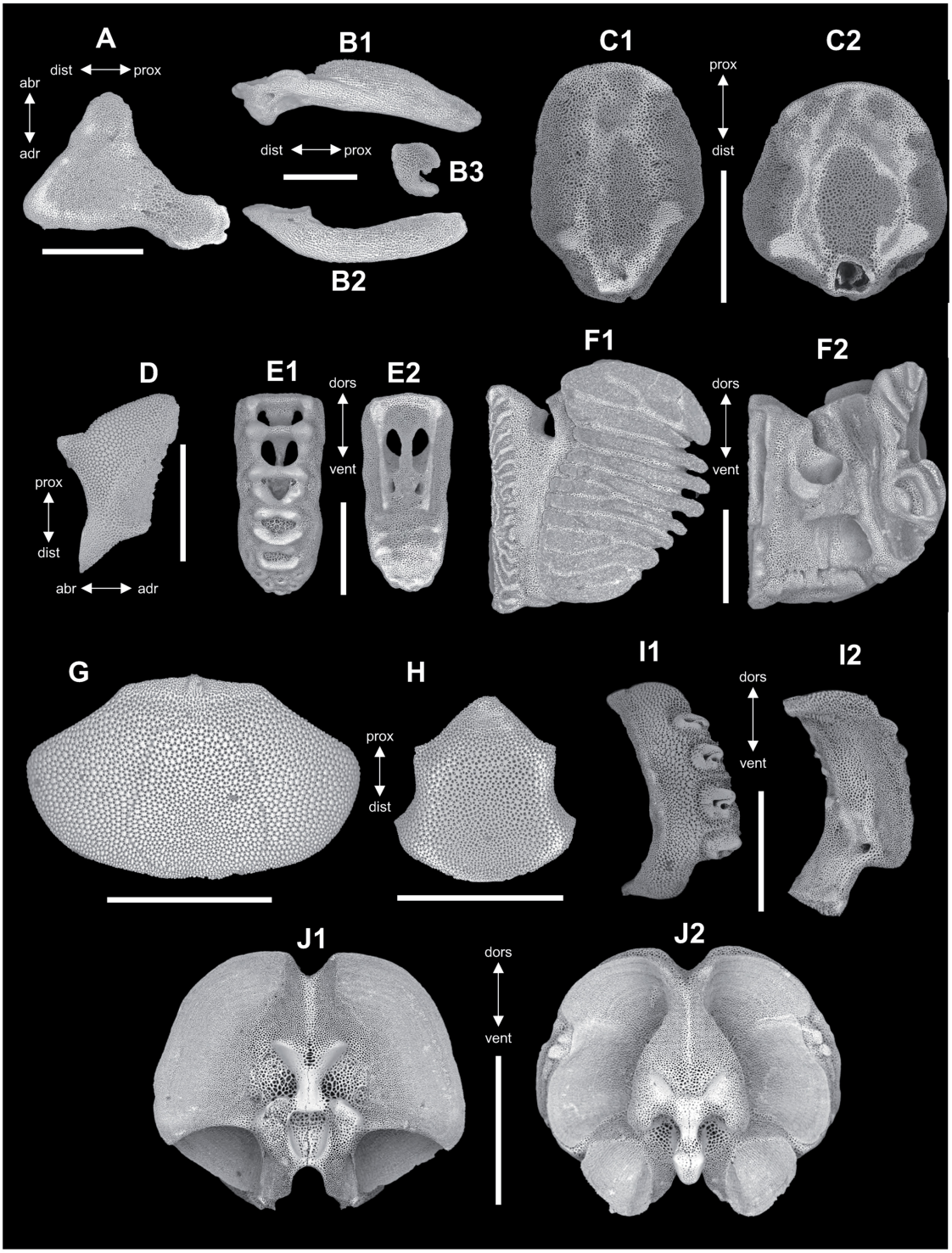

Fig. 3. SEM images of *Breviturma securis* sp. nov., paratype (NCHUZOOL 17237). **A–F**. Ossicles from disc. **A**. Radial shield. **B**. Genital plates: **B1**. Adradial genital plate. **B2**. Abradial genital plate. **B3**. Oral genital plate. **C**. Oral shields, inner view: **C1**. Normal plate. **C2**. Madreporite. **D**. Adoral shield. **E**. Dental plates: **E1**. Outer view. **E2**. Inner view. **F**. Oral plates: **F1**. Abradial view. **F2**. Adradial view. **G–J**. Ossicles from proximal arm. **G**. Dorsal arm plate. **H**. Ventral arm plate. **I**. Lateral arm plates: **I1**. Outer view. **I2**. Inner view. **J**. Vertebrae: **J1**. Proximal view. **J2**. Distal view. Abbreviations: abr = abradial; adr = adradial; dist = distal; dors = dorsal; prox = proximal; vent = ventral. Scale bars = 1 mm.

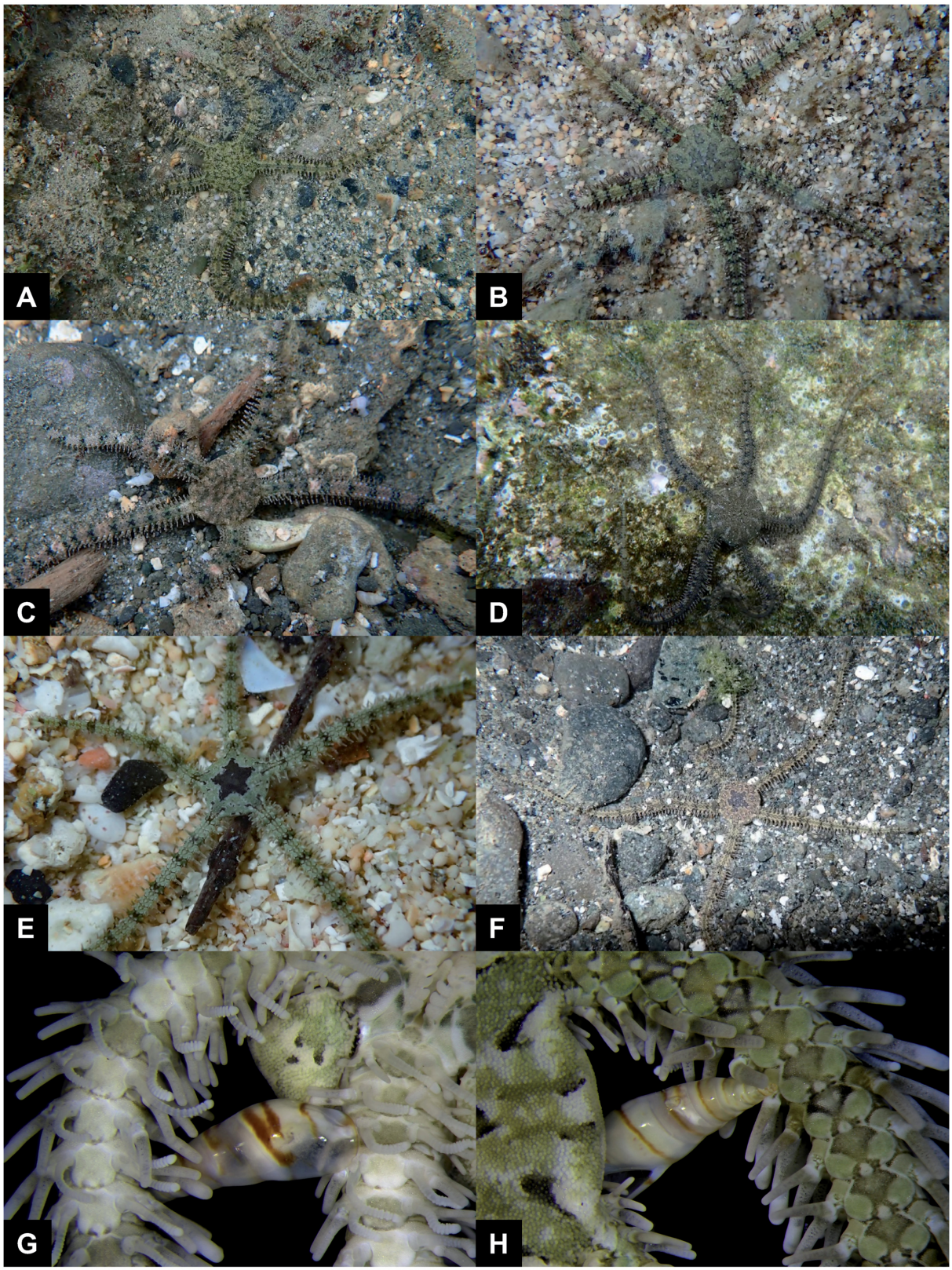

Fig. 4. *Breviturma securis* sp. nov. **A–F**. In situ. **A–D**. Adults. **E–F**. Juveniles. **G–H**. A specimen (NCHUZOOL 17241) with a parasitic snail (Eulimidae sp.) attached at the base of an arm. **G**. Ventral view. **H**. Dorsal view.

of dorsal arm plates lower in young individuals, higher in larger specimens (Fig. 5C). Four arm spines from proximal arm segments in almost all examined specimens, five arm spines in only two specimens. Second dorsalmost arm spines from 15th–18th arm segment of most large individuals prominently elongated, swollen, absent in smaller individuals (Fig. 5D). For the detailed results, see Morphological analyses on *Breviturma securis* sp. nov.

Coloration

In life, the dorsal disc and ventral interradial areas exhibit a yellowish-gray to greenish-gray coloration, variegated with lighter and darker patches. These regions are adorned with discontinuous short dark lines that never form a reticular pattern (Figs 2A, 4A–D). In juveniles, a dark 'star' may occasionally appear at the center of the disc but never connects to the arm base (Fig. 4E–F). Dorsal arm plates share the disc's background color but feature a dark 'axe-shaped' pattern in the center, the 'axe bit' is at proximal side and the 'axe poll' is at the distal side (Fig. 2E). Darker plates occur every two to three segments on both the dorsal and ventral arm plates, giving the arms a transversely banded appearance (Figs 2A, 4A–F). Arm spines are light gray with irregular darker annulations (Fig. 2E–F). Oral shields, jaws, and

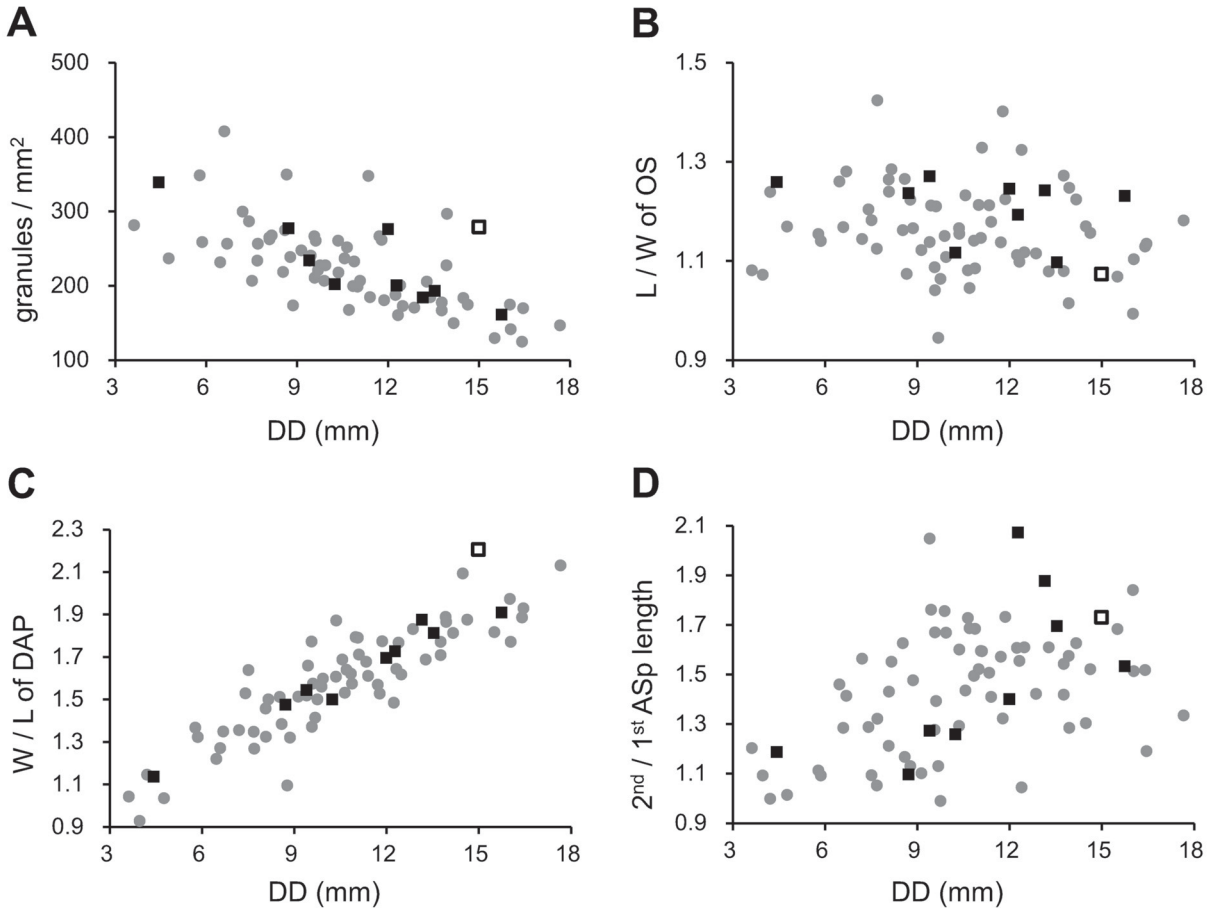

Fig. 5. Morphological measurements of *Breviturma securis* sp. nov. **A**. Granule densities on the dorsal central disc within an area of 1 mm². **B**. Length-to-width ratios of the oral shield (OS). **C**. Width-to-length ratio of the dorsal arm plates (DAP) from the 15th arm segment. **D**. Ratio of the length of the second dorsalmost arm spine (ASp) to that of the first dorsalmost arm spine at 15th arm segment. Markers: hollow squares represent the holotype; solid black squares represent paratypes; solid gray dots represent other examined specimens.

ventral arm plates are very light in color, either white or creamy yellow (Fig. 2B, D, F). Tentacle scales are white, occasionally exhibiting tiny dark dots (Fig. 2D, F). Tube feet are white (Fig. 2D, F).

Ecological and behavioral notes

This species inhabits sandy substrates beneath rocks, ranging from the intertidal zone to shallow subtidal depths of up to 8 m. It is highly sympatric with other brittle stars, including *B. dentata*, *B. krohi*, *Ophiocoma scolopendrina*, and *Amphipholis squamata* (Delle Chiaje, 1828). On one occasion, an individual was parasitized by a snail (Eulimidae sp.) attached at the base of an arm (Fig. 4G–H).

Distribution

Reunion Island; Taiwan; Papua New Guinea.

Remarks

Breviturma securis sp. nov. was previously misidentified as *B. brevipes* in Taiwan, including in academic literature (e.g., Chao *et al.* 1991) and in field guides (Hung 2000). The photographs for *B. brevipes* in those publications obviously match the new species in both morphology and coloration, showing strong arm spines, a greenish base color, variegated dark and light spots, and a conspicuous dark 'axe' pattern on the dorsal arm plates. For the same reasons, in a field guide to tropical Indo-Pacific echinoderms (Ryanskiy 2020), three records were identified as *Breviturma* sp., *Ophionereis* sp., and Ophiodermatidae sp., respectively; all should be referred to this new species. In our previous work (Shih *et al*. 2023), the new species was recorded from Lanyu, Taiwan, under the name *Breviturma* aff. *dentata* because of the presence of four strong arm spines, yet it exhibited a completely different coloration from the typical *B. dentata* (Müller & Troschel, 1842). The specimens from Lanyu are now designated as the holotype and paratypes in this study.

Furthermore, three specimens labeled as "*Ophiocoma brevipes*" archived in the NMNS (see Other material examined under *Breviturma securis* sp. nov.) were reexamined and confirmed to belong to this new species. These two species can be distinguished by their coloration and the number of AS on the proximal arm segments (see Discussion).

Breviturma krohi (Stöhr, Boissin & Hoareau, 2013)
Fig. 6

Ophiocoma (*Breviturma*) *krohi* Stöhr, Boissin & Hoareau, 2013: 17–20, figs 2g–l, 4k–o, 5c, f, i, l, o, r, 6.

Ophiocoma sp. nov. – Hoareau *et al.* 2013: 2.
Ophiocoma (*Breviturma*) *krohi* – Boissin *et al.* 2016: 283, fig. 3i.
Ophiocoma krohi – Conand *et al.* 2018: 118 (in list).
Breviturma krohi – Fortaleza *et al.* 2020: 288, fig. 3b.
Breviturma cf. *krohi* – Shih *et al.* 2023: 125 (in list).

non *Ophiocoma brevipes* Peters, 1851 – Stöhr *et al.* 2008: 553, figs 5e–f.

Diagnosis

The dorsal disc is densely covered with fine granules that extend seamlessly to the oral side. The oral shields are trapezoidal, while the adoral shields are unevenly triangular. There are four oral papillae and eight to ten tooth papillae. The dorsal arm plates are oval in shape. The arm spines are tapering, with numbers ranging from three to five; the proximal arm segments consistently have five spines. The ventral arm plates are pentagonal, each bearing two oval tentacle scales on its lateral sides. The coloration is yellowish-brown, with dark brown patterns on the dorsal disc (Fig. 6A, C, E–F). Some of these patterns

are pentamerously symmetrical, while others are uniformly dark. The central patterns on the dorsal arm plates are also dark. The arms are transversely banded (Fig. 6), with the arm spines being dark gray. On the oral side, the coloration is light, with tiny dark spots scattered across the surface (Fig. 6B, D).

Material examined

TAIWAN – **Penghu County** • 10 specs (DD = 4.03–12.17 mm); Wang'an, Dongjiyu; 23°15′24.9″ N, 119°39′59.4″ E; depth < 1 m; 22 Apr. 2024; K. Chang and Y.-C. Hsu leg.; NCHUZOOL 17274 • 1 spec. (DD = 8.68 mm); Wang'an, Dongjiyu; 23°15′24.9″ N, 119°39′59.4″ E; depth < 1 m; 24 Apr. 2024; K. Chang and Y.-C. Hsu leg.; NCHUZOOL 17275 • 5 specs (DD = 7.67–12.13 mm); Wang'an, Dongjiyu; 23°15′24.9″ N, 119°39′59.4″ E; depth < 1 m; 25 Apr. 2024; K. Chang and Y.-C. Hsu leg.; NCHUZOOL 17276 • 2 specs (DD = 10.90–11.01 mm); Wang'an, Dongyupingyu; 23°15′29.1″ N, 119°30′46.5″ E; depth 1 m; 28 Apr. 2024; K. Chang and Y.-C. Hsu leg.; NCHUZOOL 17277. – **Pingtung County** • 2 specs (DD = 6.05–9.36 mm); Siaoliouciou, Shanfu Fishery Harbor; 22°20′24.4″ N, 120°21′46.2″ E; depth < 1 m; 12 Feb. 2023; K. Chang and Y.-C. Hsu leg.; NCHUZOOL 17258 • 1 spec. (DD = 10.99 mm); Checheng, Huangjin Beach; 22°04′52.6″ N, 120°42′06.2″ E; depth < 1 m; 25 Feb. 2024; K. Chang *et al.* leg.; NCHUZOOL 17270 • 3 specs (DD = 7.27–9.12 mm); Hengchun, Houbihu; 21°56′18.9″ N, 120°44′43.6″ E; depth < 1 m; 25 Dec. 2023; K. Chang *et al.* leg.; NCHUZOOL 17269 • 2 specs (DD = 10.46–12.06 mm); Hengchun, Wanlitong; 21°59′44.4″ N 120°42′22.2″ E; depth < 1 m; 26 Feb. 2024; K. Chang *et al.* leg.; NCHUZOOL 17271 • 6 specs (DD = 3.95–12.73 mm); Hengchun, Wanlitong; 21°59′42.4″ N, 120°42′22.3″ E; depth 5 m; 28 Feb. 2024; K. Chang *et al.* leg.; NCHUZOOL 17273 • 1 spec. (DD = 12.27 mm); Mudan, Gangzaibi; 22°08′49.8″ N, 120°53′32.4″ E; depth < 1 m; 27 Feb. 2024; K. Chang *et al.* leg.; NCHUZOOL 17272. – **Taitung County** • 2 specs (DD = 6.21–9.43 mm); Chenggong, Jihuei; 23°07′00.4″ N, 121°23′50.1″ E; depth < 1 m; 11 Apr. 2023; K. Chang *et al.* leg.; NCHUZOOL 17260 • 6 specs (DD = 6.81–11.73 mm); Donghe, Dulan; 22°51′51.7″ N, 121°12′34.9″ E; depth < 1 m; 16 Oct. 2024; K. Chang *et al.* leg.; NCHUZOOL 17337 • 1 spec. (DD = 6.20 mm); Lanyu, Dongcing; 22°04′29.2″ N, 121°34′04.3″ E; depth < 1 m; 15 Mar. 2023; K. Chang *et al.* leg.; NCHUZOOL 17259 • 4 specs (DD = 9.00–12.99 mm); Lanyu, Longmen Harbor; 22°00′16.5″ N, 121°34′52.7″ E; depth 7 m; 23 May 2023; C.-H. Chang *et al.* leg.; NCHUZOOL 17261 • 3 specs (DD = 9.44–12.07 mm); Lanyu, Longmen Harbor; 22°00′16.5″ N, 121°34′52.7″ E; depth 7 m; 24 May 2023; K. Chang and Y.-C. Hsu leg.; NCHUZOOL 17262 • 1 spec. (DD = 17.17 mm); Lanyu, Langdao; 22°04′45.3″ N, 121°31′47.9″ E; depth < 1 m; 25 May 2023; K. Chang and Y.-C. Hsu leg.; NCHUZOOL 17263 • 1 spec. (DD = 13.57 mm); Lanyu, Langdao; 22°04′45.3″ N, 121°31′47.9″ E; depth < 1 m; 6 Jul. 2023; K. Chang and Y.-C. Hsu leg.; NCHUZOOL 17264 • 1 spec. (DD = 11.36 mm); Lanyu, Dongcing; 22°03′23.1″ N, 121°33′56.8″ E; depth < 1 m; 6 Jul. 2023; K. Chang *et al.* leg.; NCHUZOOL 17265 • 8 specs (DD = 4.94–13.23 mm); Lanyu, "Jimavonot" [Jade Maiden Rock]; 22°04′53.6″ N, 121°31′05.7″ E; depth 8 m; 7 Jul. 2023; K. Chang and Y.-C. Hsu leg.; NCHUZOOL 17266 • 1 spec. (DD = 15.58 mm); Lanyu, Langdao; 22°04′45.3″ N, 121°31′47.9″ E; depth < 1 m; 15 Sep. 2023; K. Chang and Y.-C. Hsu leg.; NCHUZOOL 17267 • 1 spec. (DD = 8.45 mm); Lanyu, Hongtou; 22°01′19.4″ N, 121°33′29.7″ E; depth < 1 m; 15 Sep. 15; K. Chang *et al.* leg.; NCHUZOOL 17268.

Ecological and behavioral notes

This species inhabits sandy substrates beneath rocks, ranging from the intertidal zone to shallow subtidal zone. In Taiwan, it is highly sympatric with other brittle stars, including *B. dentata*, *B. securis* sp. nov., *Ophiocoma scolopendrina*, and *Amphipholis squamata*.

Distribution

Indo-West Pacific: Reunion Island; Okinawa Islands, Japan; Taiwan; Philippines; Palau; Mariana Islands; Wake Island; Samoa; Niue; Hawaii; Society Islands, Polynesia.

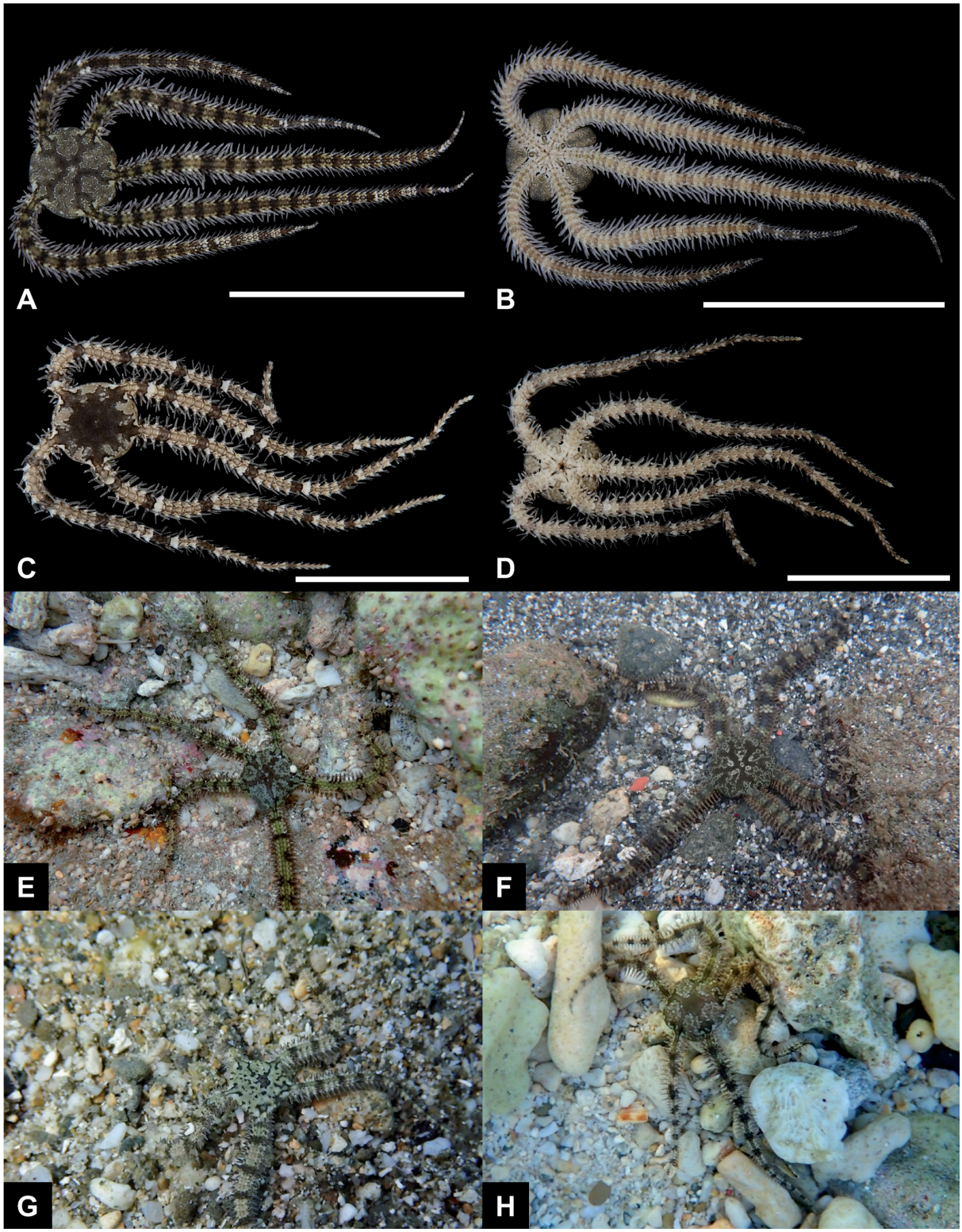

Fig. 6. *Breviturma krohi* (Stöhr, Boissin & Hoareau, 2013). **A–B**. Ethanol preserved specimen (NCHUZOOL 17274), DD = 11.40 mm. **C–D**. Ethanol preserved specimen (NCHUZOOL 17266), DD = 4.94 mm. **E–H**. *B. krohi*, in situ. Scale bars: A–B = 30 mm; C–D = 10 mm.

Remarks

Breviturma krohi with uniformly dark color pattern sometimes can be confused with *B. dentata* in appearance. While these two species can be separated using 1) the arm spine numbers from proximal arm segments, which are four or five (Stöhr *et al*. 2013; our material) (vs four in *B. dentata*); 2) the W/L ratios of dorsal arm plates, which are lower in *B. krohi* (ca 1.8) (Stöhr *et al*. 2013) (vs 2.0 in *B. dentata*); and 3) the maximum disc diameter of this species, which is 17.17 mm in our material (vs 28 mm in *B. dentata*).

Morphological analyses on Breviturma securis sp. nov.

A total of 75 specimens of *Breviturma securis* sp. nov. were examined for morphological measurements. The densities of granules ranged from 125 to 408 per mm² (N = 74, Fig. 5A). A significant negative correlation with disc diameter was observed (Pearson's r = –0.66, $p < 0.0001$), as well as a significant linear relationship (Linear Regression: $R^2 = 0.43$, $F(1, 72) = 54.98$, $p < 0.0001$). The L/W ratios of oral shields ranged from 0.95 to 1.42 (N = 76, Fig. 5B). However, no significant correlation with disc diameter was observed (Pearson's r = –0.17, $p = 0.14$). The W/L ratios of the 15th dorsal arm plates ranged from 0.93 to 2.21 (N = 75, Fig. 5C), showing a significant positive correlation with disc diameter (Pearson's r = 0.89, $p < 0.0001$) and a significant linear relationship (Linear Regression: $R^2 = 0.79$, $F(1, 73) = 270.29$, $p < 0.0001$). Finally, the ratio of the second dorsalmost arm spine length to that of the first dorsalmost arm spine in the 15th arm segment ranged from 0.99 to 2.07 (N = 75, Fig. 5D). This trait also exhibited a significant positive correlation with disc diameter (Pearson's r = 0.46, $p < 0.0001$) and a significant linear relationship (Linear Regression: $R^2 = 0.21$, $F(1, 73) = 19.12$, $p < 0.0001$).

Molecular analyses

A molecular analysis was conducted, using 39 sequences. Of these, 35 sequences of 16S and COI genes of *Breviturma* spp. were derived from our collections. Combined sequences of *B. doederleini* and the holotype of *B. krohi* were obtained from GenBank, and for each species the 16S and COI were from the same individuals. The data of *B. pusilla* were limited to COI due to the absence of the 16S gene in GenBank (Table 1).

The phylogenetic tree topology shows that species of *Breviturma* form a well-supported clade. Furthermore, both *B. securis* sp. nov. and *B. krohi* are strongly supported as distinct clades and are identified as sister species (Fig. 7). Sequences of *B. krohi* from its holotype (Bk14 and BkC14) and our collections form a unified clade (Fig. 7). The K2P nucleotide divergence distances and bp differences among species of *Breviturma* are shown in Table 2. The average intraspecific K2P distance for *B. krohi* and *B. securis* is 1.74% and 1.04%, respectively, with average bp differences of 11.23 and 6.76. The K2P distances between *B. krohi* and other congeners range from 18.27% to 26.28%, with bp differences ranging from 103.77 to 144.15. Similarly, the K2P distances between *B. securis* and other congeners range from 18.27% to 26.66%, with bp differences ranging from 104.51 to 145.27.

Discussion

Since Chao *et al.* (1991) conducted the last review of brittle stars from Taiwan, over 30 years have passed without any new records being added. One species that warrants inclusion is *Breviturma krohi*, which was described in 2013. *Breviturma krohi* was previously identified as "*Ophiocoma brevipes/doederleini*" in Stöhr *et al.* (2008) and was later confirmed as a new species in Stöhr *et al.* (2013). In the original description, the holotype had four arm spines at the proximal arm segments, while the paratypes had either four or five arm spines in equal proportion (Stöhr *et al.* 2013). However, in our collections, all specimens with a DD greater than 10 mm have five arm spines. Despite these morphological differences,

Table 2. Matrix of percentage pairwise nucleotide divergences with K2P distances and mean numbers of nucleotide differences based on COI gene within and between species of *Breviturma* Stöhr, Boissin & Hoareau, 2013 used in this study. Values of the ranges are shown in parentheses.

	intraspecific	**interspecific**						
		B. brevipes	***B. dentata***	***B. doederleini***	***B. krohi***	***B. pica***	***B. pusilla***	***B. securis*** sp. nov.
neucleotide divergence								
B. krohi	1.74 (0.46–3.46)	20.25 (19.66–20.76)	20.26 (19.36–21.90)	19.35 (18.95–19.62)		21.49 (20.90–22.55)	26.28 (25.56–26.94)	18.27 (16.71–19.44)
B. securis sp. nov.	1.04 (0.15–1.71)	21.54 (20.68–22.40)	18.73 (17.54–19.80)	22.47 (21.88–23.05)	18.27 (16.71–19.44)	22.27 (21.72–22.79)	26.66 (26.13–27.06)	
nucleotide difference								
B. krohi	11.23 (3–22)	114.65 (112–117)	115.21 (111–123)	103.77 (102–105)		121.85 (119–127)	144.15 (141–147)	104.51 (97–110)
B. securis sp. nov.	6.76 (1–11)	121.05 (117–125)	107.83 (102–113)	117.55 (115–120)	104.51 (97–110)	125.55 (123–128)	145.27 (143–147)	

our combined 16S and COI sequences clearly form a clade with that of the holotype of *B. krohi*, supporting our identification (Fig. 7).

For *B. securis* sp. nov., several morphological traits strongly indicate its placement within the family Ophiocomidae (O'Hara *et al.* 2018), including the granule-covered disc (Fig. 2C), the entire dental plate (Fig. 3E), the presence of tooth papillae and oral papillae (Fig. 2D), and the freestanding arm spines (Fig. 2A–B, E–F). The finely granulated disc (Fig. 2C) further suggests its placement within the genus *Breviturma* (Stöhr *et al*. 2013). *Breviturma securis* can be distinguished from *B. longispina*, *B. paucigranulata*, *B. pica*, and *B. pusilla* (i.e., Devaney's "*pica* group") by its arm spines morphology. For the first three species, the arm spines are tapering and elongated (Devaney 1970, 1974), while in *B. pusilla*, they are fragile and hollow, with the upper second arm spines from the 10th to 12th arm segments embedded in transparent soft tissue, giving them a clavate appearance (Brock 1888; Koehler 1905; Devaney 1970; Liao 2004). In contrast, *B. securis* has thicker and shorter arm spines than any of above species. Compared with the species of Deaveny's "*brevipes* group", *B. securis* differs from *B. brevipes* and *B. doederleini* by 1) the number of arm spines at proximal arm segments being four (vs five in *B. brevipes* and *B. doederleini*); 2) its yellowish and greenish coloration (Figs 2, 4) (vs white or whitish-gray in *B. brevipes* and dark brown or black in *B. doederleini*) (Table 3). Compared with

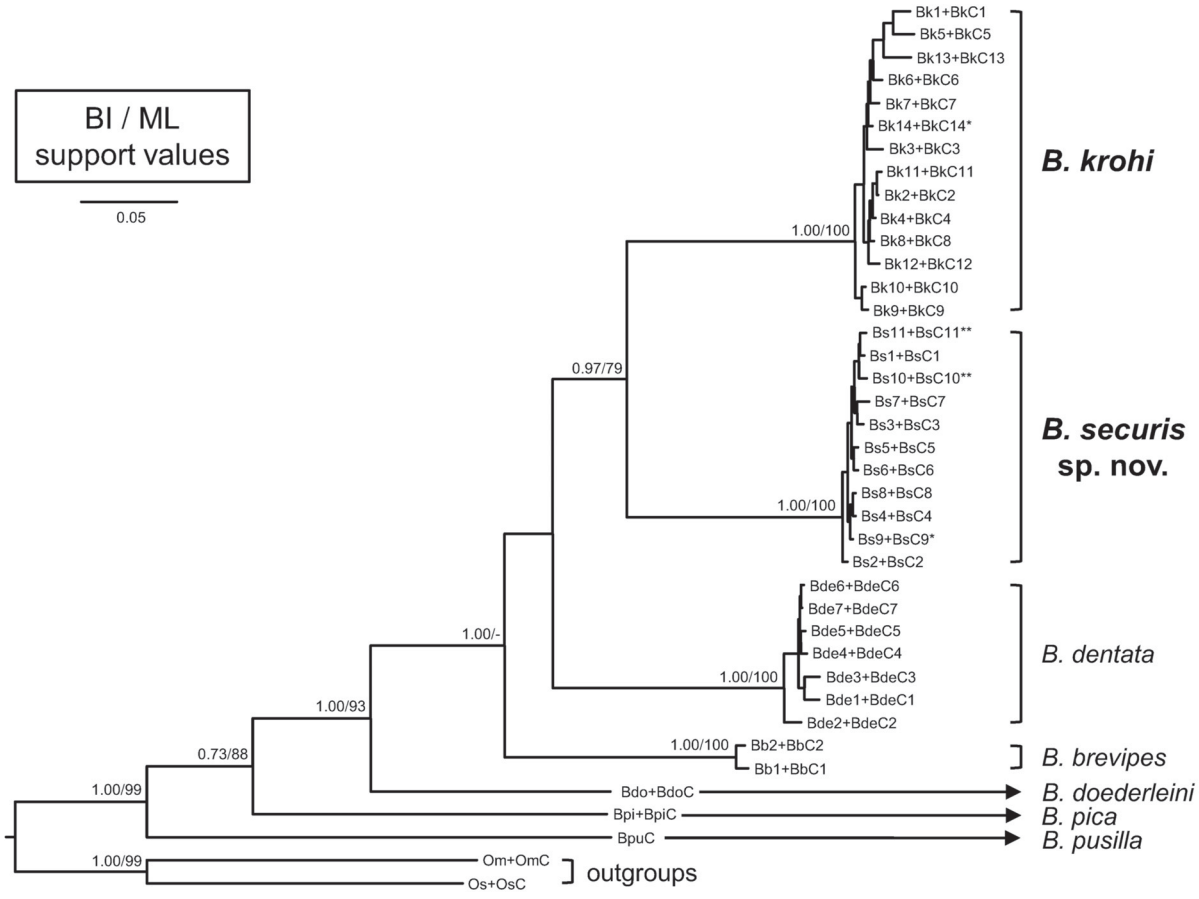

Fig. 7. A Bayesian inference (BI) phylogenetic tree for species of *Breviturma* Stöhr, Boissin & Hoareau, 2013 from the Indo-West Pacific, based on the 16S rRNA and cytochrome c oxidase subunit (COI) genes. Support values at the nodes represent the posterior probability from BI and bootstrap value from maximum likelihood (ML). Only values above 70% are shown. For haplotype names and GenBank accession numbers, see Table 1. * = holotype; ** = paratype.

Table 3. Morphological comparison of selected species of *Breviturma* Stöhr, Boissin & Hoareau, 2013. All characteristics were taken from the original descriptions of each species unless marked with an asterisk (*), in which case they were referred from the review by Stöhr *et al.* (2013).

	B. securis sp. nov.	***B. brevipes***	***B. dentata***	***B. doederleini***	***B. krohi***
Maximum DD (mm)	17.7	19.7*	28.0*	31.0	15.5
DAP	elliptical	oval	elliptical	elliptical	oval
DAP W / L ratio	2.2	2	2*	3	1.8
Base color	yellowish-gray or greenish-gray	whitish-green or yellowish-white	brown	light brown black*	yellowish-brown
Dorsal disc pattern	variegated with dark and light patches	brownish or greenish marbling	uniformly or marbled brown*; reticulated*; spotted*	small black dots; dark reticulating*	large patches; irregular spots; star-shaped radiation; mottled; uniformly dark brwon
ASp on proximal arm	4	5	4 or 5*	5	4 or 5
ASp annulation	weak	absent	absent	strong	weak
Source	this study	Peters (1851), Stöhr *et al.* (2013)	Müller & Troschel (1842), Stöhr *et al.* (2013)	De Loriol (1899), Stöhr *et al.* (2013)	Stöhr *et al.* (2013)

B. dentata, *B. securis* can be delimited by 1) the maximum DD, which is 17.65 mm (vs 28 mm in *B. dentata*); 2) its yellowish and greenish coloration (Figs 2, 4) (vs dark brown or black with dotted or reticular pattern in *B. dentata*) (Table 3). Additionally, *B. krohi*, which has similar appearance and maximum size as *B. securis*, can be differentiated by 1) the second dorsalmost arm spine from the 15th–18th arm segments of adult *B. securis* are always elongated and have swollen tips, which are absent in *B. krohi*; 2) the color pattern of *B. securis* is more variegated and broken (Figs 2A, C, 4A–D), in contrast to the uniformly colored and pentamerous radial patterns of *B. krohi* (Fig. 6A, C, E–F, H); and 3) the dorsal arm plates of *B. securis* are wider than those of *B. krohi* (Table 3).

The validity of *B. securis* sp. nov. is further supported by COI sequences, also known as DNA barcodes (Hajibabaei *et al.* 2007; Hoareau & Boissin 2010). The interspecific K2P distances of COI between *B. securis* and its congeners range from 18.27–26.66% (Table 2). These results are consistent with previous studies on other brittle stars, which reported a mean value of 20.64% for 15 genera (34 species) (Ward *et al.* 2008) and a mean value of 18.9% for 13 genera (42 species) from the southwestern Indian Ocean (Boissin *et al.* 2017).

Additionally, in the phylogenetic analyses based on the combined 16S+COI sequences (Fig. 7), *B. securis* sp. nov. forms a strongly supported clade and is sister to another well-supported clade of *B. krohi*, confirming the validity of both species, which together form a major clade.

Regarding the distribution range of *B. securis* sp. nov., the confirmed areas so far are Taiwan's main island and its offshore islets. However, some images in a field guide by Ryanskiy (2020) likely represent this species and are labeled with locations such as Reunion Island and Papua New Guinea. Considering the distribution patterns of other species of *Breviturma*, which are widely distributed across the Indo-West Pacific and even reach the South Pacific (Devaney 1970, 1974; Clark & Rowe 1971; Stöhr *et al.* 2013), the distribution range of *B. securis* is expected to extend throughout the Indo-West Pacific.

Acknowledgments

This study was supported by grants from the National Science and Technology Council (NSTC 112-2313-B-005-051-MY3) and the Ocean Conservation Administration, Ocean Affairs Council (project no. 111-C-71), Executive Yuan, Taiwan. We gratefully acknowledge the Marine National Park Headquarters (permit no. 1131002861) and the Kenting National Park Headquarters (permit no. 1121280057) for granting collection permissions. Special thanks go to the members of HTS's lab for their assistance with specimen collection, Prof. Chiou-Rong Sheue for her support with SEM photography, and Kwen-Shen Lee for facilitating the loan of specimens from the NMNS. We acknowledge two anonymous referees who greatly improved this manuscript.

References

Applegate AL. 1984. Echinoderms of southern Taiwan. *Zoological Studies* 23: 93–118.

Boissin E., Hoareau T.B., Paulay G. & Bruggemann J.H. 2016. Shallow-water reef ophiuroids (Echinodermata: Ophiuroidea) of Réunion (Mascarene Islands), with biogeographic considerations. *Zootaxa* 4098: 273–297. https://doi.org/10.11646/zootaxa.4098.2.4

Boissin E., Hoareau T.B., Paulay G. & Bruggemann J.H. 2017. DNA barcoding of reef brittle stars (Ophiuroidea, Echinodermata) from the southwestern Indian Ocean evolutionary hot spot of biodiversity. *Ecology and Evolution* 7: 11197–11203. https://doi.org/10.1002/ece3.3554

Brock J. 1888. Die Ophiuridenfauna des indischen Archipels. *Zeitschrift für wissenschaftliche Zoologie* 47: 465–539. Available from https://www.biodiversitylibrary.org/page/49595866 [accessed 5 May 2025].

Chao S.-M. 2002. The shallow-water echinoderms from Lanyu, Taiwan. *Collection and Research* 15: 1–7.

Chao S.-M., Chen C.-P. & Chang K.-H. 1991. Some shallow-water ophiurans (Echinodermata: Ophiuroidea) of Taiwan. *Zoological Studies* 30: 117–126.

Clark A.M. & Rowe F.W.E. 1971. *Monograph of Shallow-Water Indo-West Pacific Echinoderms*. Trustees of the British Museum (Natural History), London.

Conand C., Ribes-Beaudemoulin S., Trentin F., Mulochau T. & Boissin E. 2018. Marine biodiversity of La Reunion Island: Echinoderms. *Western Indian Ocean Journal of Marine Science* 17: 111–124.

De Loriol P. 1899. Notes pour servir à l'étude des échinodermes. *Mémoires de la Société de Physique et d'Histoire naturelle de Genève* 33: 1–34. https://www.biodiversitylibrary.org/page/36246661

Devaney D.M. 1970. *Studies on Ophiocomid Brittlestars. I. A New Genus (Clarkcoma) of Ophiocominae with a Reevaluation of the Genus Ophiocoma*. Smithsonian Institution Press, Washington. https://doi.org/10.5479/si.00810282.51

Devaney D.M. 1974. Shallow-water echinoderms from British Honduras, with a description of a new species of *Ophiocoma* (Ophiuroidea). *Bulletin of Marine Science* 24: 122–164.

Fortaleza M.A., Lanutan J.J., Consuegra J.M. & Nañola C.L. Jr 2020. Diversity of echinoderms in intertidal and shallow-water areas of Samal Island, Philippines. *Philippine Journal of Science* 150 (S1): 281–297. https://doi.org/10.56899/150.S1.19

Hajibabaei M., Singer G.A., Hebert P.D. & Hickey D.A. 2007. DNA barcoding: How it complements taxonomy, molecular phylogenetics and population genetics. *Trends in Genetics* 23: 167–172. https://doi.org/10.1016/j.tig.2007.02.001

Hoareau T.B. & Boissin E. 2010. Design of phylum-specific hybrid primers for DNA barcoding: Addressing the need for efficient COI amplification in the Echinodermata. *Molecular Ecology Resources* 10: 960–967. https://doi.org/10.1111/j.1755-0998.2010.02848.x

Hoareau T.B., Boissin E., Paulay G. & Bruggemann J.H. 2013. The Southwestern Indian Ocean as a potential marine evolutionary hotspot: Perspectives from comparative phylogeography of reef brittle-stars. *Journal of Biogeography* 40: 2167–2179. https://doi.org/10.1111/jbi.12155

Huang H.-D. & Lee K.-S. 2021. *Echinoderms of South Penghu Marine National Park*. Marine National Park Headquarters, Kaohsiung, Taiwan. [In Chinese.]

Hung K.-H. 2000. *Common Marine Organisms in Penghu*. Culture Affairs Bureau, Penghu County, Taiwan. [In Chinese.]

Kimura M. 1980. A simple method for estimating evolutionary rates of base substitutions through comparative studies of nucleotide sequences. *Journal of Molecular Evolution* 16: 111–120. https://doi.org/10.1007/BF01731581

Koehler R. 1905. Ophiures de l'expédition du Siboga. Part 2. Ophiures littorales. *Siboga-Expeditie* 45b: 1–140. Available from https://www.biodiversitylibrary.org/page/2219486 [accessed 5 May 2025].

Kumar S., Stecher G., Suleski M., Sanderford M., Sharma S. & Tamura K. 2024. MEGA12: Molecular Evolutionary Genetic Analysis version 12 for adaptive and green computing. *Molecular Biology and Evolution* 41: 1–9. https://doi.org/10.1093/molbev/msae263

Lanfear R., Frandsen P.B., Wright A.M., Senfeld T. & Calcott B. 2017. PartitionFinder 2: New methods for selecting partitioned models of evolution for molecular and morphological phylogenetic analyses. *Molecular Biology and Evolution* 34: 772–773. https://doi.org/10.1093/molbev/msw260

Liao Y. 2004. *Fauna Sinica Phylum Echinodermata, Class Ophiuroidea.* Science Press, Beijing. [In Chinese.]

Minh B.Q., Schmidt H.A., Chernomor O., Schrempf D., Woodhams M.D., Haeseler A. von & Lanfear R. 2020. IQ-TREE 2: New models and efficient methods for phylogenetic inference in the genomic era. *Molecular Biology and Evolution* 37: 1530–1534. https://doi.org/10.1093/molbev/msaa015

Müller J.H. & Troschel F.H. 1842. *System der Asteriden*. F. Vieweg & Sohn, Braunschweig. https://doi.org/10.5962/bhl.title.11715

O'Hara T.D., Hugall A.F., Thuy B., Stöhr S. & Martynov A.V. 2017. Restructuring higher taxonomy using broad-scale phylogenomics: The living Ophiuroidea. *Molecular Phylogenetics and Evolution* 107: 415–430. https://doi.org/10.1016/j.ympev.2016.12.006

O'Hara T.D., Stöhr S., Hugall A.F., Thuy B. & Martynov A. 2018. Morphological diagnoses of higher taxa in Ophiuroidea (Echinodermata) in support of a new classification. *European Journal of Taxonomy* 416: 1–35. https://doi.org/10.5852/ejt.2018.416

O'Hara T.D., Hugall A.F., Cisternas P.A., Boissin E., Bribiesca-Contreras G., Sellanes J., Paulay G. & Byrne M. 2019. Phylogenomics, life history and morphological evolution of ophiocomid brittlestars. *Molecular Phylogenetics and Evolution* 130: 67–80. https://doi.org/10.1016/j.ympev.2018.10.003

Palumbi S.R., Martin A., Romano S., Mcmillan W.O., Stice L. & Grabowski G. 1991. *The Simple Fool's Guide to PCR*. Version 2. University of Hawaii, Honolulu, HI, USA.

Peters W. 1851. Übersicht der an der Küste von Mossambique eingesammelten Ophiuren, unter denen sich zwei neue Gattungen befinden. *Bericht über die zur Bekanntmachung geeigneten Verhandlungen der Königlich Preussischen Akademie der Wissenschaften zu Berlin* 1851: 463–466. Available from https://www.biodiversitylibrary.org/page/11056575 [accessed 5 May 2025].

Ronquist F., Teslenko M., Van Der Mark P., Ayres D.L., Darling A., Höhna, S., Larget B., Liu L., Suchard M.A. & Huelsenbeck J.P. 2012. MrBayes 3.2: Efficient Bayesian phylogenetic inference and model choice across a large model space. *Systematic Biology* 61: 539–542. https://doi.org/10.1093/sysbio/sys029

Ryanskiy A. 2020. *Starfishes and other Echinoderms of the Tropical Indo-Pacific*. Published by Andrey Ryanskiy.

SAS Institute Incorporation. 2013. SAS/STAT Software. Version 9.4. SAS Institute Incorporation, Cary, NC, USA.

Shih H.-T., Chiu Y.-W., Chang K., Wu H.-J., Hsu J.-W. & Lee K.-S. 2023. *100 Species of Marine Invertebrates in Lanyu*. Ocean Conservation Administration, Kaohsiung, Taiwan. [In Chinese.]

Stöhr S., Conand C. & Boissin E. 2008. Brittle stars (Echinodermata: Ophiuroidea) from La Réunion and the systematic position of *Ophiocanops* Koehler, 1922. *Zoological Journal of the Linnean Society* 153: 545–560. https://doi.org/10.1111/j.1096-3642.2008.00401.x

Stöhr S., Boissin E. & Hoareau T.B. 2013. Taxonomic revision and phylogeny of the *Ophiocoma brevipes* group (Echinodermata, Ophiuroidea), with description of a new subgenus (*Breviturma*) and a new species. *European Journal of Taxonomy* 68: 1–26. https://doi.org/10.5852/ejt.2013.68

Ward R.D., Holmes B.H. & O'Hara T.D. 2008. DNA barcoding discriminates echinoderm species. *Molecular Ecology Resources* 8: 1202–1211. https://doi.org/10.1111/j.1755-0998.2008.02332.x

Manuscript received: 28 October 2024
Manuscript accepted: 5 March 2025

Published on: 6 June 2025
Topic editor: Magalie Castelin
Section editor: Didier VandenSpiegel
Desk editor: Pepe Fernández

Printed versions of all papers are deposited in the libraries of four of the institutes that are members of the *EJT* consortium: Muséum national d'Histoire naturelle, Paris, France; Meise Botanic Garden, Belgium; Royal Museum for Central Africa, Tervuren, Belgium; Royal Belgian Institute of Natural Sciences, Brussels, Belgium. The other members of the consortium are: Natural History Museum of Denmark, Copenhagen, Denmark; Naturalis Biodiversity Center, Leiden, the Netherlands; Museo Nacional de Ciencias Naturales-CSIC, Madrid, Spain; Leibniz Institute for the Analysis of Biodiversity Change, Bonn – Hamburg, Germany; National Museum of the Czech Republic, Prague, Czech Republic; The Steinhardt Museum of Natural History, Tel Aviv, Israël.